



# A Methane Mechanism for Oxy-Fuel Combustion: Extinction Experiments, Model Validation, and Kinetic Analysis

Liming Cai<sup>1</sup> · Stephan Kruse<sup>1</sup> · Daniel Felsmann<sup>1</sup> · Heinz Pitsch<sup>1</sup>

Received: 4 December 2019 / Accepted: 7 April 2020 / Published online: 7 May 2020  
© Springer Nature B.V. 2020

## Abstract

While fuel combustion in oxygen-enriched environments provides a number of significant advantages, such as reduced nitrogen oxide emissions and high carbon dioxide purity for carbon sequestration, it is characterized by different physico-chemical oxidation behavior than combustion in air. Compared to nitrogen, carbon dioxide has different specific heat and effective Lewis number, and is chemically more active. Therefore, chemical mechanisms developed for the oxidation of fuel/air mixtures can fail to predict targets of interest for oxy-combustion accurately. In this study, a chemical mechanism of methane, which has been previously validated with data from experiments using air, is evaluated in terms of its prediction accuracy at oxy-conditions by comparing against available literature data. The validation takes various combustion properties into account, including ignition delay times, laminar burning velocities, and extinction strain rates, and covers a wide range of experimental conditions with respect to temperature, pressure, equivalence ratio, and carbon dioxide concentration. As additional targets, extinction strain rates of non-premixed oxy-methane flames are determined in a counterflow burner at conditions, where literature data have not yet been reported. The extensive validation demonstrates that the mechanism is able to describe oxy-methane combustion with reasonable prediction accuracy. For further insights into the underlying kinetics of diffusion flames of methane in oxy-atmosphere compared to its oxidation in air, reaction path and sensitivity analyses are performed using the validated mechanism. Notable differences between both combustion regimes are observed in the branching ratios of H-abstraction reactions by OH and H radicals and in the consumption channels of singlet methylene, which is a key species in the formation of polycyclic aromatic hydrocarbons.

**Keywords** Oxy-methane combustion · Chemical mechanism · Counterflow flame · Extinction strain rate

**Electronic supplementary material** The online version of this article (<https://doi.org/10.1007/s10494-020-00138-w>) contains supplementary material, which is available to authorized users.

✉ Liming Cai  
lcai@itv.rwth-aachen.de

<sup>1</sup> Institute for Combustion Technology, RWTH Aachen University, Templergraben 64, 52056 Aachen, Germany

## 1 Introduction

Oxy-fuel combustion is one of the most promising technologies for carbon dioxide capture. The lack of nitrogen in the fuel/oxidizer mixture leaves as combustion products mainly carbon dioxide and water, from which the  $\text{CO}_2$  can be easily separated. However, oxy-fuel combustion in  $\text{O}_2/\text{CO}_2$  environment exhibits different characteristics, in comparison to air fueled combustion. First, for equal  $\text{O}_2$  fractions, the maximum flame temperatures are substantially lower in oxy-fuel combustion, owing to the higher specific heat of  $\text{CO}_2$ . Second, the excess  $\text{CO}_2$  can participate in chemical reactions either as a reactant or as a third body for collision, affecting the fuel consumption and pollutant formation pathways. Therefore, chemical mechanisms developed for the oxidation of fuels in air may fail to predict target properties of oxy-fuel combustion accurately.

With the growing interest in oxy-combustion, a number of studies (Hargis and Petersen 2015; Koroglu et al. 2016; Pryor et al. 2017; Chen et al. 2007; Kishore et al. 2008; Benedetto et al. 2009; Mazas et al. 2010; de Persis et al. 2013; Chan et al. 2015; Kim et al. 2016; Maruta et al. 2007; Li et al. 2014) have experimentally investigated combustion of methane in oxygen-enriched environments, since methane is the main component of natural gas and coal devolatilization products. Ignition delay times of methane were measured under oxy-fuel conditions in shock tubes by Hargis and Petersen (2015), Koroglu et al. (2016), and Pryor et al. (2017). Laminar burning velocities of methane with different levels of  $\text{CO}_2$  dilution were determined with flat flame burners (Kishore et al. 2008; Mazas et al. 2010; Chan et al. 2015), in a cylindrical vessel (Benedetto et al. 2009), and in a spherical chamber (de Persis et al. 2013). For extinction limits of diffusion flames, which are important indicators for flame stability, experimental results were reported by Maruta et al. (2007) and Li et al. (2014).

While these studies revealed large differences between the combustion behavior of methane in air and oxy-atmosphere, none of them has focused on the development of chemical mechanisms giving satisfactory results under both conditions. In many of these works, chemical models available in the literature, which had only been validated against experiments using air, were employed to predict the respective experiments in oxygen and carbon dioxide atmosphere. Even though these comparisons provide partial validations of the applied chemical mechanisms for certain targets, a comprehensive model validation is missing for oxy-methane combustion.

Therefore, the purpose of this study is to propose a chemical mechanism, which is capable of predicting methane oxidation in both air and oxy-environments with high accuracy and thus enables the computational fluid dynamics modeling of complex combustion devices fueled mainly with methane running at such conditions. Instead of developing a completely new chemical model, a mechanism validated previously for methane/air oxidation (Cai et al. 2019a) is evaluated in terms of its prediction capability for oxy-methane combustion by comparing against available literature data and, if necessary, will be modified for improved accuracy. In order to assess the model reliability comprehensively for various combustion modes, the validation considers different experimental targets including ignition delay times, laminar burning velocities, and extinction strain rates measured over a wide range of initial conditions. As additional targets, extinction strain rates of diffusion flames with  $\text{CH}_4/\text{CO}_2$  fuel and  $\text{O}_2/\text{CO}_2$  oxidizer streams were determined experimentally as part of this study in a counterflow burner at conditions where flame extinction has not yet been investigated. Using the validated mechanism, the underlying kinetics of oxy-methane flames are explored based on reaction path and sensitivity analyses.

The presentation of the paper is organized as follows. First, the evaluated chemical mechanism is introduced along with the computational details. Then, the applied counterflow burner setup and the performed measurements are described. Following this, the model validation is presented and the results of sensitivity and reaction path analyses are discussed.

## 2 Chemical Mechanism and Computational Details

The chemical mechanism developed in our previous study (Cai et al. 2019a) is examined regarding its performance for oxy-methane combustion. This mechanism was proposed originally by Blanquart et al. (2009) to describe the oxidation of a set of  $C_0$ – $C_4$  hydrocarbon fuels including methane. In a series of subsequent studies, the mechanism was refined by incorporating the hydrogen mechanism from Burke et al. (2012) and extended to include the reaction schemes of polycyclic aromatic hydrocarbon (PAH) growth (Narayanaswamy et al. 2010) and nitrogen oxide formation (Cai and Pitsch 2015). It has also served as the base chemistry module of a set of chemical mechanisms of biofuel compounds (Cai et al. 2017a, 2019b, c) as well as surrogate components of gasoline and jet fuels (Cai et al. 2019a; Cai and Pitsch 2015; Narayanaswamy et al. 2016). While this mechanism has been extensively validated for the combustion of fuels in air, it has not yet been validated for experiments using  $O_2/CO_2$  as oxidizer. Note that various chemical mechanisms (Frenklach et al. 1999; Metcalfe et al. 2013; San Diego 2014) are available in the literature for methane oxidation. Selected comparisons of their performances can be found in our previous study (Cai et al. 2017b). A comprehensive discussion of these other mechanisms is beyond the scope of this study.

Oxy-methane combustion has been investigated experimentally in several literature studies. Table 1 summarizes the literature datasets used as validation targets in this work. These measurements cover a range of pressures, temperatures, equivalence ratios, and  $CO_2$  concentrations and form a database for the validation of chemical mechanisms for oxy-methane oxidation. Numerical calculation of these properties were performed using the appropriate modules in the FlameMaster (Pitsch 1990) code.

## 3 Extinction Experiments in Counterflow Burner

The extinction experiments of Maruta et al. (2007) and Li et al. (2014) were carried out for non-premixed flames with  $CH_4/CO_2$  flowing against  $O_2/CO_2$  streams with  $CO_2$  mole fractions in the oxidizer streams of 0.60 and 0.65, which lead to flame temperatures similar to those of methane/air flames. For a comprehensive model validation, the extinction limits of oxy-methane diffusion flames were measured in this study at conditions of higher  $CO_2$  concentrations in the oxidizer flows.

In the employed counterflow burner, the fuel and oxidizer flows are introduced through two opposed vertical ducts with diameters of 27.6 mm. The nozzle separation distance  $L$  is 13.75 mm. Both flows are shrouded by a nitrogen gas stream injected through a 5 mm wide ring around the nozzles. The nozzles feature an area contraction ratio of 9. Honeycombs are located in the wider section of each nozzle and serve as flow straighteners. Screens are mounted 1 mm and 5 mm upstream of the nozzle exits to achieve homogeneous top-hat velocity profiles. K-type thermocouples are located close to the nozzle exits to detect the gas stream

**Table 1** Summary of experimental measurements

Mixtures	Facilities	X <sub>CO<sub>2</sub></sub>	Conditions	References
<i>Ignition delay times</i>				
CH <sub>4</sub> /O <sub>2</sub> /N <sub>2</sub> /CO <sub>2</sub>	Shock tube	0.25	1.75 atm, $\phi = 0.5$ , X <sub>N<sub>2</sub></sub> = 0.50	Hargis and Petersen (2015)
		0.50	1.75 atm, $\phi = 0.5$ , X <sub>N<sub>2</sub></sub> = 0.25	
		0.75	1.75 and 10 atm, $\phi = 0.5$ , X <sub>N<sub>2</sub></sub> = 0	
CH <sub>4</sub> /O <sub>2</sub> /Ar/CO <sub>2</sub>	Shock tube	0.30	0.77 and 3.92 atm, $\phi = 0.5$ , X <sub>Ar</sub> = 0.61	Koroglu et al. (2016)
		0.30	0.76 and 3.77 atm, $\phi = 1.0$ , X <sub>Ar</sub> = 0.60	
		0.30	0.70 and 3.58 atm, $\phi = 2.0$ , X <sub>Ar</sub> = 0.56	
		0.60	0.61 atm, $\phi = 1.0$ , X <sub>Ar</sub> = 0.30	
		0.30	8 atm, $\phi = 1.0$ , X <sub>Ar</sub> = 0.595	
CH <sub>4</sub> /O <sub>2</sub> /Ar/CO <sub>2</sub>	Shock tube	0.60	1 and 8 atm, $\phi = 1.0$ , X <sub>Ar</sub> = 0.295	Pryor et al. (2017)
		0.30		
		0.85	30 atm, $\phi = 1.0$ , X <sub>Ar</sub> = 0	
<i>Laminar burning velocities</i>				
CH <sub>4</sub> /O <sub>2</sub> /N <sub>2</sub> /CO <sub>2</sub>	Flat flame burner	0.20, 0.40, and 0.60 <sup>1</sup>	1 bar, 307 K, X <sub>O<sub>2</sub></sub> /X <sub>O<sub>2</sub>+N<sub>2</sub></sub> = 0.21	Kishore et al. (2008)
	Cylindrical vessel	0.20	1 bar, 300 K, X <sub>O<sub>2</sub></sub> /X <sub>O<sub>2</sub>+N<sub>2</sub></sub> = 0.21 and 0.40	Di Benedetto et al. (2009)
		0.40	1 bar, 300 K, X <sub>O<sub>2</sub></sub> /X <sub>O<sub>2</sub>+N<sub>2</sub></sub> = 0.40	
		0.60	1 bar, 300 K, X <sub>O<sub>2</sub></sub> /X <sub>O<sub>2</sub>+N<sub>2</sub></sub> = 0.80	
CH <sub>4</sub> /O <sub>2</sub> /CO <sub>2</sub>	Flat flame burner	0.20 and 0.40	1 atm, 373 K	Mazas et al. (2010)
	Spherical chamber	0.29 and 0.40 <sup>1</sup>	1 atm, 300 K, $\phi = 0.7$	de de Persis et al. (2013)

Table 1 (continued)

Mixtures	Facilities	$X_{\text{CO}_2}$	Conditions	References
$\text{CH}_4/\text{O}_2/\text{N}_2/\text{CO}_2$	Flat flame burner	0.10 and 0.15 <sup>1</sup>	1 atm, 298 K, $X_{\text{O}_2}/X_{\text{O}_2+\text{N}_2} = 0.21$	Chan et al. (2015)
<i>Extinction strain rates</i>				
Fuel: $\text{CH}_4/\text{CO}_2$	Counterflow burner	0.60 and 0.65 <sup>3</sup>	2, 5, and 7 bar, $L^4 = 4.3$ mm, $T_1 = T_2 = 300$ K <sup>5</sup>	Maruta et al. (2007)
Oxidizer: $\text{O}_2/\text{CO}_2$		0.60 and 0.65 <sup>3</sup>	1, 2, and 5 bar, $T_1 = T_2 = 300$ K, $L = 10$ mm	
Fuel: $\text{CH}_4/\text{CO}_2$	Counterflow burner	0.60 and 0.65 <sup>3</sup>	1 bar, $L = 12$ mm, $T_1 = 300$ K,	Li et al. (2014)
Oxidizer: $\text{O}_2/\text{CO}_2$			$T_2 = 300, 700, \text{ and } 1000$ K,	

<sup>1</sup>  $X_{\text{CO}_2} = X_{\text{CO}_2}/(X_{\text{CO}_2} + X_{\text{CH}_4})$ .

<sup>2</sup>  $X_{\text{O}_2} : X_{\text{He}} : X_{\text{CO}_2} = 0.3 : 0.2 : 0.5$ .

<sup>3</sup>  $\text{CO}_2$  mole fraction in the oxidizer stream.

<sup>4</sup> Distance between nozzles.

<sup>5</sup>  $T_1$ : Temperature of the fuel stream;  $T_2$ : Temperature of the oxidizer stream

temperatures. All mass flow controllers are operated by a Lab-View based control-software and have an accuracy of 0.8% of adjusted flows and 0.2% of full-scale flow rates. Concerning these accuracies, Monte-Carlo simulations were performed to quantify the uncertainties of the mixture compositions and the strain rate. For a level of confidence of 95%, the uncertainty in the measured extinction strain rate is below 3% and that in the fuel mass fraction is below 5% for all measured conditions. The characteristic strain rate of the oxidizer at the stagnation plane is defined according to Seshadri and Williams (1978) as

$$a_2 = \frac{2|v_2|}{L} \left( 1 + \frac{|v_1| \sqrt{\rho_1}}{|v_2| \sqrt{\rho_2}} \right). \quad (1)$$

Here,  $v_1$  and  $v_2$  indicate the exit velocities of fuel and oxidizer streams, respectively. The densities of fuel and oxidizer flows are denoted by  $\rho_1$  and  $\rho_2$ , respectively. In the experiments, the nozzle exit velocities were increased stepwise until extinction, while keeping the flows in momentum balance. The corresponding strain rate at extinction was recorded as the extinction strain rate. The present measurements were carried out at atmospheric pressure for fuel and oxygen mass fractions of 0.15–0.50 and 0.210–0.233, respectively. The exact compositions can be found in Table 2. The temperatures of the fuel and oxidizer streams were 300 and 310 K, respectively.

## 4 Mechanism Validation

The mechanism performance for the new and the literature data is presented in this section. Figures 1, 2 and 3 show the comparisons of the model predictions with the ignition delay time data from Hargis and Petersen (2015), Koroglu et al. (2016), and Pryor et al. (2017), respectively. Hargis and Petersen (2015) determined the ignition delay times of lean  $\text{CH}_4/\text{O}_2/\text{N}_2/\text{CO}_2$  mixtures for various  $\text{N}_2/\text{CO}_2$  ratios over a temperature range of 1450–1900 K at pressures of 1.75 and 10 atm. Koroglu et al. (2016) performed experiments at a similar temperature range for  $\text{CH}_4/\text{O}_2/\text{CO}_2$  mixtures in bath gas of Ar. The measurements were carried out at pressures of 0.61–3.92 atm for equivalence ratios of 0.5, 1.0, and 2.0 and for  $\text{CO}_2$  loadings of 30% and 60% by mole. Datasets at higher pressures and for higher  $\text{CO}_2$  loadings were reported by Pryor et al. (2017). As shown in Figs. 1, 2 and 3, the model predicts the shock tube data from both experiments satisfactorily.

Laminar burning velocities of  $\text{CH}_4/\text{O}_2/\text{N}_2/\text{CO}_2$  and  $\text{CH}_4/\text{O}_2/\text{CO}_2$  mixtures have been reported in a number of literature studies. Kishore et al. (2008) measured the burning velocities of  $\text{CH}_4/\text{air}/\text{CO}_2$  mixtures in a flat flame burner over a range of equivalence ratios of 0.8–1.3 for three different blending ratios of  $\text{CH}_4/\text{CO}_2$  ( $X_{\text{CO}_2}/(X_{\text{CO}_2} + X_{\text{CH}_4}) = 0.2, 0.4, \text{ and } 0.6$ ). Benedetto et al. (2009) investigated the flame speeds of stoichiometric  $\text{CH}_4/\text{O}_2/\text{N}_2/\text{CO}_2$  mixtures in a cylindrical vessel for varying  $\text{CO}_2$  mole fractions and  $\text{O}_2/\text{N}_2$  ratios. The laminar flame speeds of  $\text{CH}_4/\text{O}_2/\text{CO}_2$  mixtures with  $\text{CO}_2$  mole fractions of 20 and 40% were determined by Mazas et al. (2010) in a flat flame burner at an initial temperature of 373 K. Experimental data of a lean  $\text{CH}_4/\text{O}_2/\text{N}_2/\text{CO}_2$  mixture with an equivalence ratio of 0.7 were reported by de Persis et al. (2013) for  $X_{\text{CO}_2}/(X_{\text{CO}_2} + X_{\text{CH}_4})$  of 0.29 and 0.40. The last dataset considered in the validation was taken from Chan et al. (2015), who experimentally determined the flame speeds of  $\text{CH}_4/\text{air}/\text{CO}_2$  mixtures in a flat flame burner for  $X_{\text{CO}_2}/(X_{\text{CO}_2} + X_{\text{CH}_4})$  of 0.10 and 0.15. The measured laminar burning velocities are compared in Fig. 4 with those calculated by using the present mechanism. The model predicts the experiments satisfactorily for most

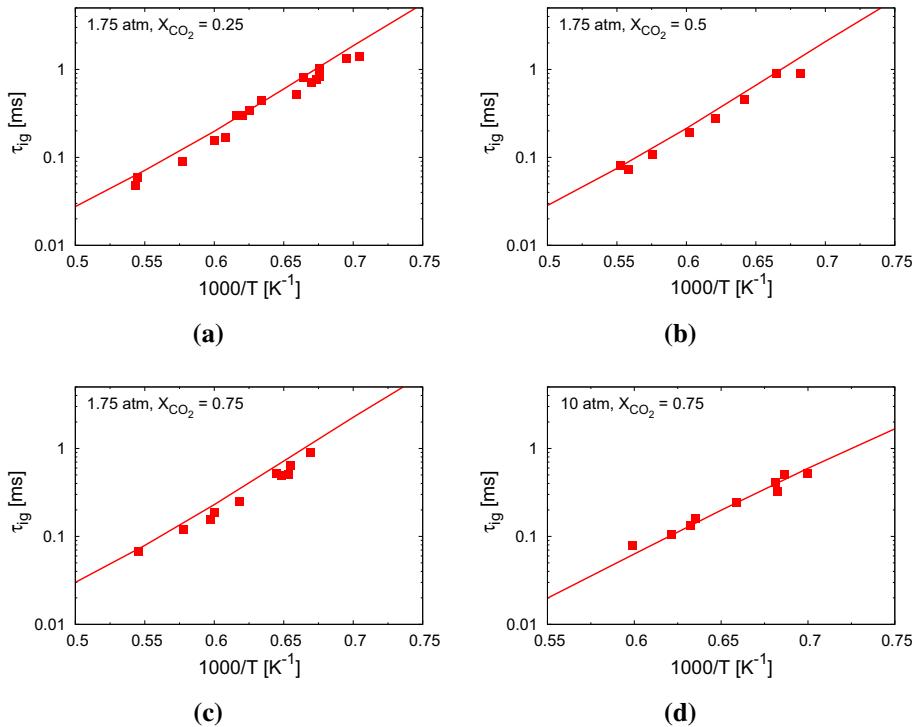


**Fig. 1** Ignition delay times of  $\text{CH}_4/\text{O}_2/\text{N}_2/\text{CO}_2$  mixtures with an equivalence ratio of 0.5. Symbols denote the experimental data from Hargis and Petersen (2015) and lines show the computed results

**Table 2** Oxidizer ( $\text{O}_2/\text{CO}_2$ ) and fuel ( $\text{CH}_4/\text{CO}_2$ ) stream compositions in experiments

$Y_{\text{O}_2,2}$	$Y_{\text{F},1}$
0.210	0.250–0.500
0.225	0.150–0.275
0.233	0.200–0.400

investigated conditions. Note that all of these data were reported at atmospheric pressure and, except that of Mazas et al. (2010), at a temperature of roughly 300 K. Experimental observations at elevated pressures and temperatures are of high interest for further mechanism validation, but are, however, lacking in the literature.

The extinction strain rates of diffusion flames with  $\text{CH}_4/\text{CO}_2$  flowing against  $\text{O}_2/\text{CO}_2$  streams were measured by Maruta et al. (2007) and Li et al. (2014). As mentioned earlier, both studies were conducted for flames with large oxygen mole fractions in the oxidizer streams, which have thus maximum temperatures similar to methane/air flames. While Maruta et al. (2007) performed experiments at ambient temperatures and studied the influence of pressure and nozzle distance on the flame extinction limits, Li et al. (2014) quantified experimentally the impact of varying oxidizer stream temperatures. The results of Maruta et al. (2007) and Li et al. (2014) are presented in Figs. 5 and 6, respectively, in comparison with the corresponding numerical results. While the model predicts the data of Maruta et al. (2007) with reasonable accuracy, it overpredicts the experiments of Li et al.

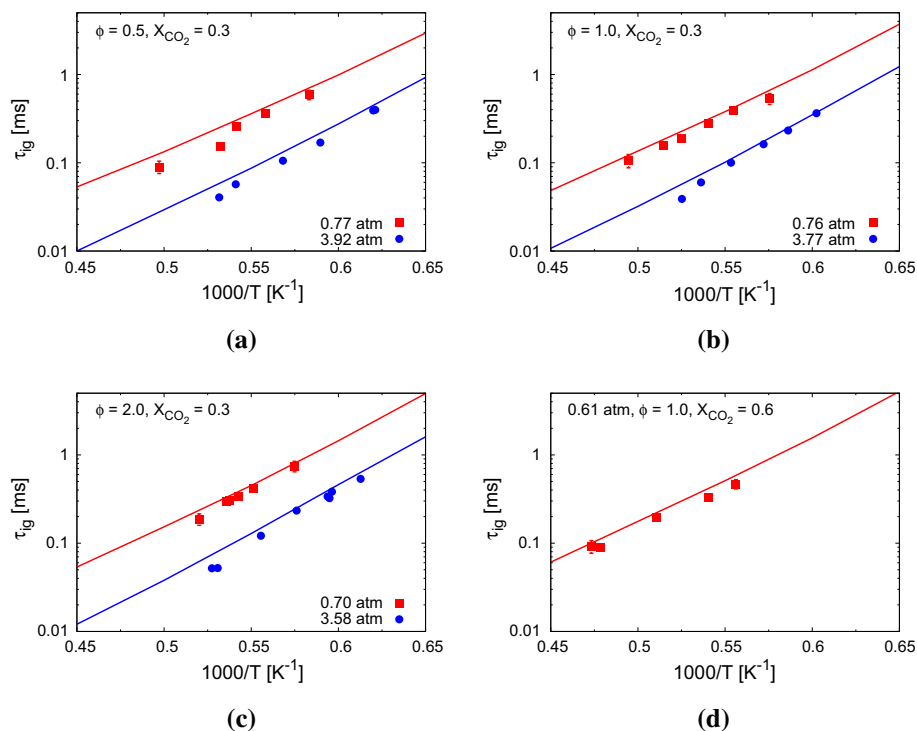


**Fig. 2** Ignition delay times of  $\text{CH}_4/\text{O}_2/\text{Ar}/\text{CO}_2$  mixtures. Symbols denote the experimental data from Koroglu et al. (2016) and lines show the computed results

(2014) by a factor of more than two. It is worth mentioning that a disagreement is observed between those data of Maruta et al. (2007) and Li et al. (2014) that were reported as similar conditions, as shown in Fig. 7. Figure 8 shows the extinction strain rates determined experimentally in the present study. For conditions with low oxygen concentrations, the model matches the data well.

## 5 Reaction Path and Sensitivity Analyses

The controlling kinetics of premixed oxy-methane mixtures in homogeneous reactors and laminar flames have been explored in literature studies (Hargis and Petersen 2015; Koroglu et al. 2016; Chen et al. 2007; Kishore et al. 2008; Benedetto et al. 2009; Mazas et al. 2010; de Persis et al. 2013; Chan et al. 2015). It was commonly found that the presence of  $\text{CO}_2$  strongly increases the reverse rate of the reaction of  $\text{CO} + \text{OH} \rightleftharpoons \text{CO}_2 + \text{H}$ , which is the most important heat release reaction in the oxidation of hydrocarbon fuels. This study focuses on the reaction kinetics of diffusion flames. Sensitivity analyses are first discussed for flame stability in terms of the maximum flame temperature  $T_{\max}$ . The sensitivity coefficient ( $S_i$ ) of the elementary reaction  $i$  is defined as  $A_i/T_{\max} \cdot \partial T_{\max} / \partial A_i$ . Here,  $A_i$  is the pre-exponential factor of the reaction. Positive sensitivity coefficients characterize reactions, which enhance the heat release and thus increase the flame



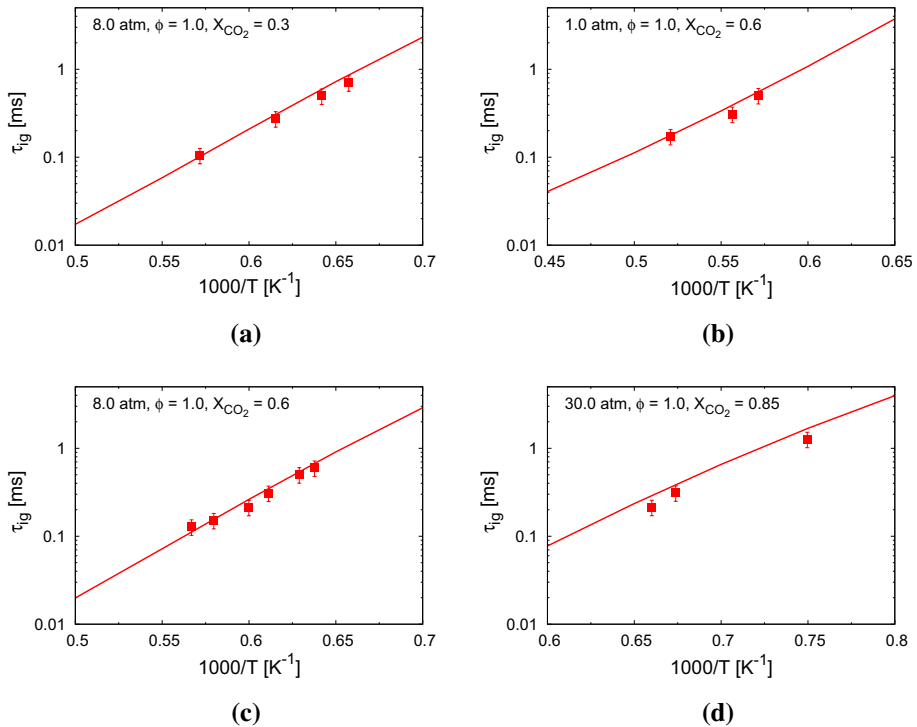


**Fig. 3** Ignition delay times of  $CH_4/O_2/Ar/CO_2$  mixtures. Symbols denote the experimental data from Pryor et al. (2017) and lines show the computed results

temperature. Reactions with negative coefficients decrease the flame temperature and promote flame extinction.

The sensitivity analyses were conducted for a flame with  $CH_4/CO_2$  fuel and  $O_2/CO_2$  oxidizer streams with  $Y_{F,1} = 0.35$ ,  $Y_{O_2,2} = 0.233$ , and  $a_2 = 210$  1/s. For comparison of the oxidation kinetics at this oxy-condition with those in nitrogen atmosphere, sensitivity analyses were also performed for a  $CH_4/N_2$  versus  $O_2/N_2$  flame with  $Y_{F,1} = 0.35$ ,  $Y_{O_2,2} = 0.233$ , and  $a_2 = 423$  1/s. Both flames are close to extinction limits and have almost identical maximum flame temperatures. Thus, the thermodynamic effect on the flame kinetics is minimized in this comparison.

The results are presented in Fig. 9. As expected, the most important chain-branching reaction  $H + O_2 \rightleftharpoons O + OH$  shows the largest sensitivity in both flames. Comparing the results of the two flames, most reactions exhibit decreased sensitivities at the oxy-fuel condition. In particular, the importance of the reaction  $CO + OH \rightleftharpoons H + CO_2$  is reduced significantly, which can be attributed to the promoting effect of higher  $CO_2$  concentration on its backward rate. Two reactions show larger sensitivities at the oxy-fuel condition. First, the reaction between singlet methylene ( $CH_2(S)$ ) and  $CO_2$  is enhanced due to the large concentration of  $CO_2$  in oxy-environment. As indicated by its negative sensitivity, this reaction contributes to a temperature decrease. Second, the H-abstraction of

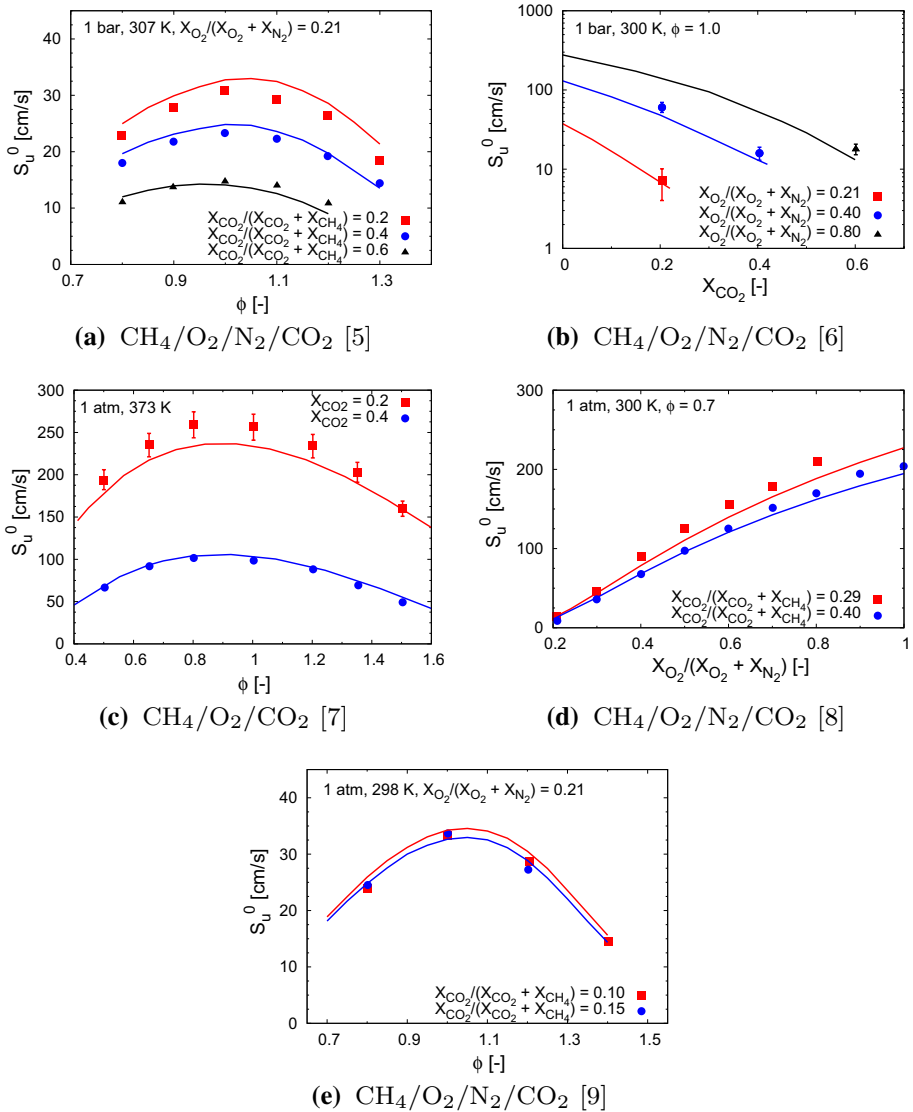


**Fig. 4** Laminar burning velocities of oxy-methane combustion. Symbols and lines denote the measured and computed results, respectively

methane by OH radical is of slightly increased importance in oxy-atmosphere as well. As the amount of available H radicals in the oxy-flame is lower owing to the reaction of H with  $\text{CO}_2$ , the H-abstraction by H radical is retarded and conversely the abstraction by OH radical is advanced.

For further understanding of the effects of the  $\text{CO}_2$  enrichment on the methane consumption channels, reaction path analyses were carried out for both flames at the same conditions as in the presented sensitivity analyses. Results are shown in Fig. 10. In the oxy-flame, 35% and 54% of methane are consumed by the build-up of H and OH radicals,

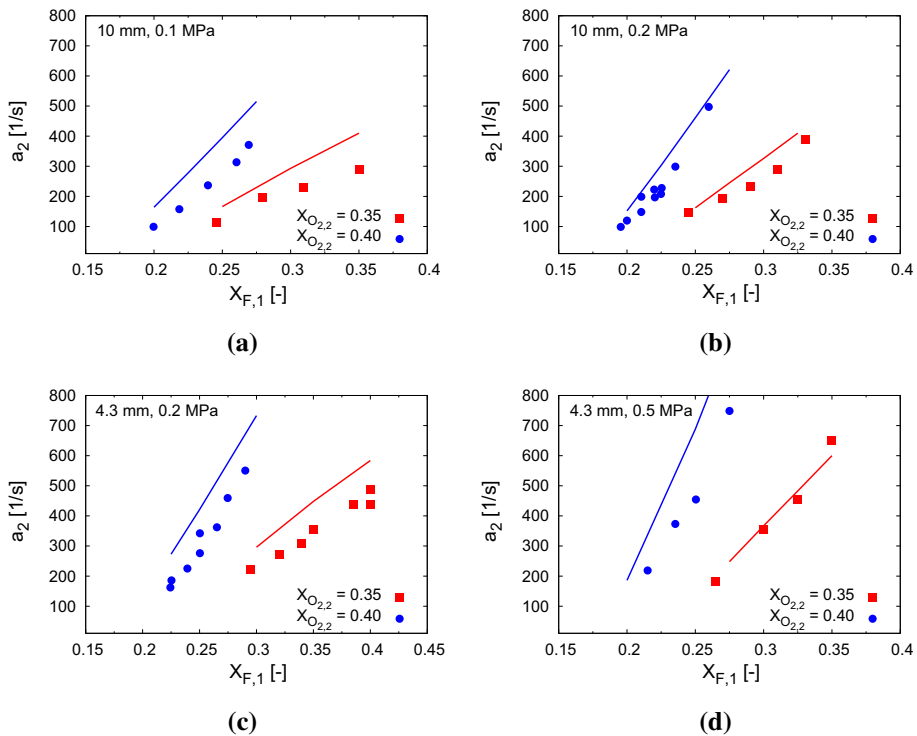


**Fig. 5** Extinction strain rate of diffusion flames with  $\text{CH}_4/\text{CO}_2$  (300 K) flowing against  $\text{O}_2/\text{CO}_2$  (300 K) streams. Symbols denote measurements (Maruta et al. 2007) and lines show the computed results

respectively. The direct product, the methyl radical, can react with the O radical, yielding either formaldehyde ( $\text{CH}_2\text{O}$ ) and H radical or  $\text{H}_2$ , CO, and H radicals. Alternatively, two methyl radicals can recombine to form ethane, from which an H-atom is abstracted by H,  $\text{CH}_3$ , or OH radicals to produce an ethyl radical. The ethyl radical undergoes subsequent reaction steps to form triplet methylene ( $\text{CH}_2(\text{T})$ ). This reaction sequence of ethane  $\rightarrow$  ethyl radical  $\rightarrow$  ethylene  $\rightarrow$  vinyl radical  $\rightarrow$  acetylene  $\rightarrow$  triplet methylene, however, barely affects the flame temperature, as indicated by the small sensitivities of these reaction steps. The methyl radical can also undergo reaction with OH radicals to produce singlet methylene, whose consumption channels have notable influence on the flame temperature.  $\text{CH}_2(\text{S})$  can either react with  $\text{CO}_2$  yielding formaldehyde or isomerize to  $\text{CH}_2(\text{T})$ . Through the H-atom abstraction of  $\text{CH}_2(\text{T})$ , the methylidyne (CH) radical is produced, which is subsequently oxidized to formyl radical. The formyl radical decomposes to carbon monoxide, and the final product, carbon dioxide, is then formed via the reaction of  $\text{CO} + \text{OH} \rightleftharpoons \text{CO}_2 + \text{H}$ .

Compared with the air-fueled flame, the H-atom abstraction by OH radical becomes more favorable in the oxy-flame. An increase of the branching ratios of H-abstraction reactions by OH and H radicals can be observed for various reaction steps in Fig. 10, e.g., for the H-abstraction reactions of methyl radicals, formaldehyde, ethane, and ethylene. As described earlier, the large concentration of  $\text{CO}_2$  increases the rate of the backward reaction of  $\text{CO} + \text{OH} \rightleftharpoons \text{H} + \text{CO}_2$ , leading to a decreased amount of available H radicals in the oxy-flame and consequently inhibiting the H-atom abstraction by H radical. In addition, the

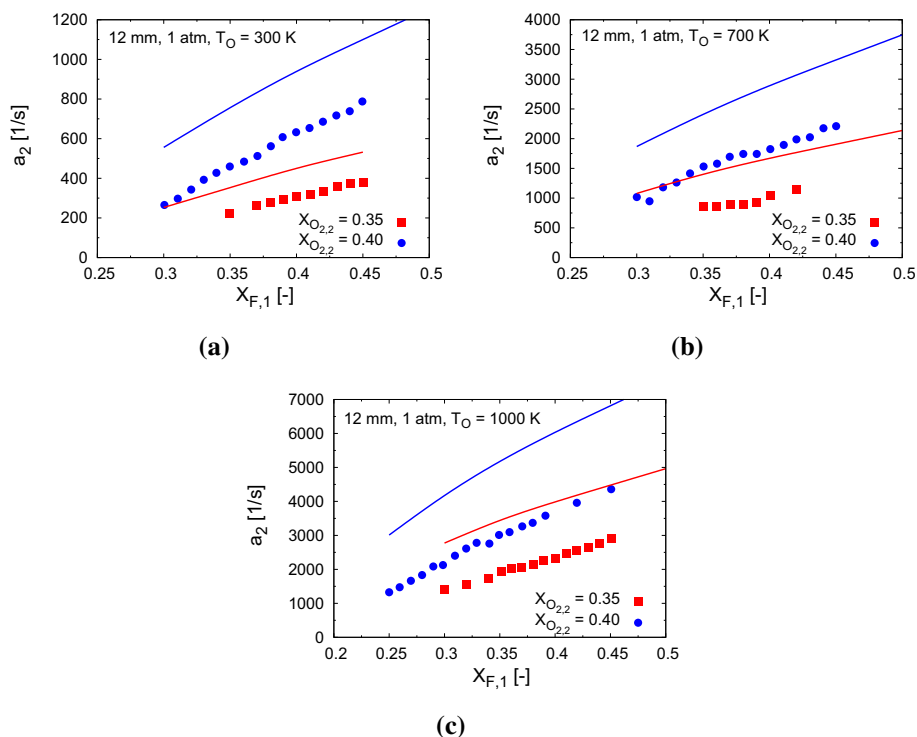
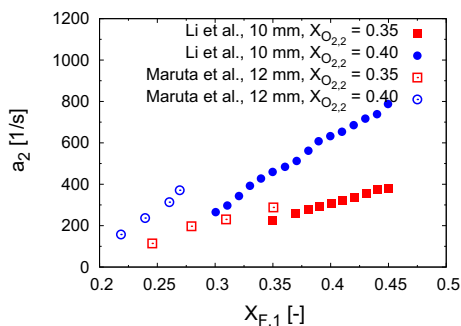


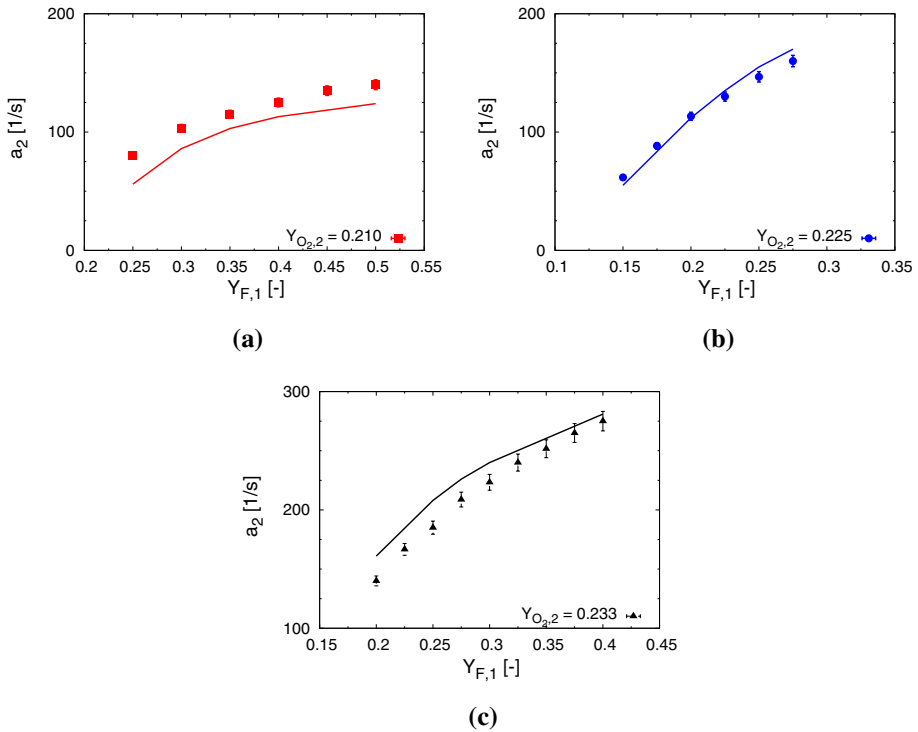
**Fig. 6** Extinction strain rates of diffusion flames with  $\text{CH}_4/\text{CO}_2$  (300 K) flowing against  $\text{O}_2/\text{CO}_2$  streams. Symbols denote measurements (Li et al. 2014) and lines show the computed results

**Fig. 7** Extinction strain rates of diffusion flames with  $\text{CH}_4/\text{CO}_2$  (300 K) flowing against  $\text{O}_2/\text{CO}_2$  (300 K) streams. Symbols denote measurements (Maruta et al. 2007; Li et al. 2014)



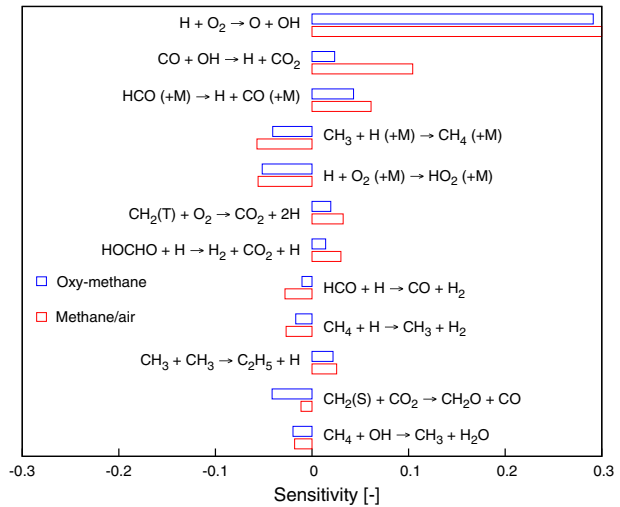
consumption channels of singlet methylene are also significantly different between the two flames. Under the air condition, 68% of singlet methylene isomerizes to triplet methylene with a third body of either nitrogen or water. In the oxy-environment, the absence of nitrogen suppresses the reaction of  $\text{CH}_2(\text{S}) + \text{N}_2 \rightleftharpoons \text{CH}_2(\text{T}) + \text{N}_2$  completely. Instead, the reaction of  $\text{CH}_2(\text{S})$  with  $\text{CO}_2$  is favored, which decreases the maximum flame temperature and increases extinction propensity.

The aforementioned changes in reaction pathways affect not only the flame stability but also the formation of PAH and their precursors. For instance, in the air-fueled flame, 43%



**Fig. 8** Extinction strain rates of diffusion flames with  $CH_4/CO_2$  (300 K) flowing against  $O_2/CO_2$  (310 K) streams. Symbols denote measurements and lines show the computed results

**Fig. 9** Sensitivity analyses of  $CH_4/CO_2$  versus  $O_2/CO_2$  ( $Y_{F,1} = 0.35$ ,  $Y_{O_2,2} = 0.233$ , and  $a_2 = 210$  1/s) and  $CH_4/N_2$  versus  $O_2/N_2$  ( $Y_{F,1} = 0.35$ ,  $Y_{O_2,2} = 0.233$ , and  $a_2 = 423$  1/s) flames. Red and blue values indicate the results for flames in air and oxy-atmosphere, respectively



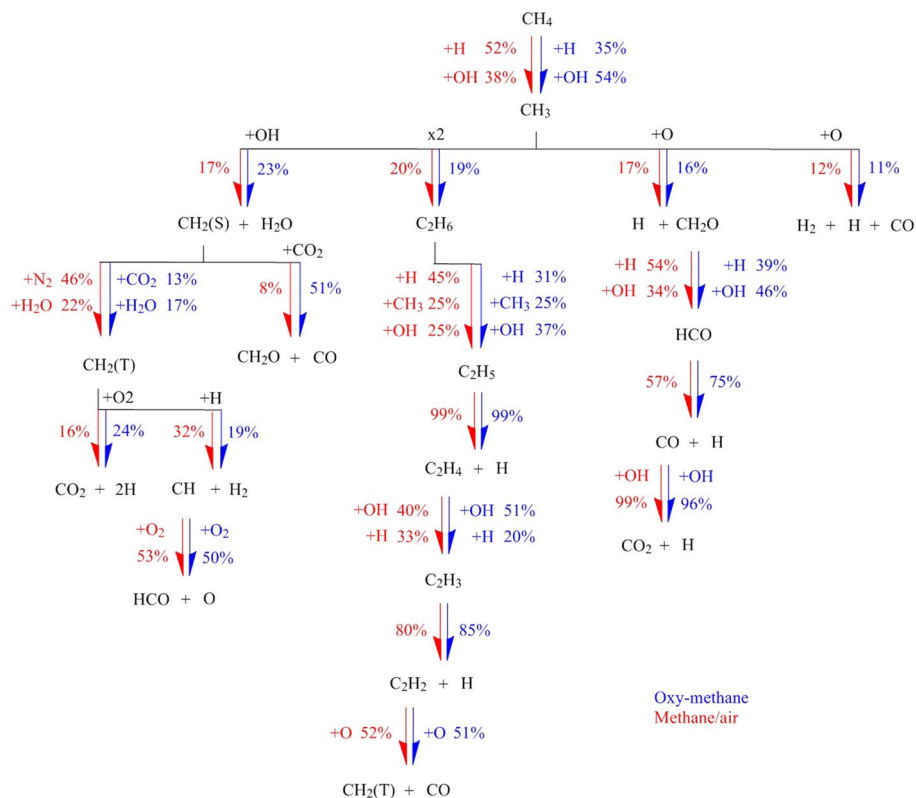


**Fig. 10** Reaction flux analyses of  $\text{CH}_4/\text{CO}_2$  versus  $\text{O}_2/\text{CO}_2$  ( $Y_{\text{F},1} = 0.35$ ,  $Y_{\text{O}_2,2} = 0.233$ , and  $a_2 = 210$  l/s) and  $\text{CH}_4/\text{N}_2$  versus  $\text{O}_2/\text{N}_2$  ( $Y_{\text{F},1} = 0.35$ ,  $Y_{\text{O}_2,2} = 0.233$ , and  $a_2 = 423$  l/s) flames. Red and blue values indicate the results for flames in air and oxy-atmosphere, respectively

and 22% of the propargyl radicals are formed via the reaction of  $\text{CH}_2(\text{S}) + \text{C}_2\text{H}_2 \rightleftharpoons \text{C}_3\text{H}_3 + \text{H}$  and the H-abstraction reaction of propyne by H radical, respectively. Both reactions are inhibited in the oxy-flame, leading to a decreased production of propargyl radicals.

## 6 Conclusion

A chemical mechanism, which had been validated previously for methane/air oxidation, was validated extensively in this study against literature and new experimental data under oxy-conditions and is demonstrated to predict the combustion targets accurately for most investigated conditions. It is worth mentioning that this mechanism also contains the detailed chemistry of PAH and  $\text{NO}_x$  formation, allowing the prediction of pollutant emissions of oxy-methane combustion in computational fluid dynamic simulation, for which the performance requires nevertheless further exploration. The mechanism is available as Supplementary Material. As part of this study, the extinction strain rates of counterflow flames with  $\text{CH}_4/\text{CO}_2$  fuel and  $\text{O}_2/\text{CO}_2$  oxidizer streams were experimentally determined at conditions, where literature observation is lacking, and serve as additional validation targets. Using the validated mechanism, reaction path and sensitivity analyses were performed

to understand the controlling kinetics of oxy-methane diffusion flames. The branching ratios between H-abstraction reactions by OH and H radicals were found to be strongly increased in comparison with combustion in air. The promotion of the backward reaction of  $\text{CO} + \text{OH} \rightleftharpoons \text{H} + \text{CO}_2$  due to the high  $\text{CO}_2$  concentration reduces the amount of available H radicals in the system and thus inhibits the H-abstraction reactions by H radicals at oxy-conditions. In addition, it is also highlighted that the diffusion flame stability is considerably more sensitive to the consumption channels of singlet methylene at oxy-conditions than in air.

**Acknowledgements** This work was performed as part of the collaborative research center SFB/Transregio 129 “Oxyflame”, which is funded by the German Research Foundation (DFG). The authors would like to thank Mr. Kiran K. Yalamanchi for his support with numerical calculations.

## Compliance with Ethical Standards

**Conflict of interest** This study was funded by the German Research Foundation (DFG). The authors declare that they have no conflict of interest.

## References

- Benedetto, A.D., Cammarota, F., Sarli, V., Russo, G., Salzano, E.: Explosion behavior of  $\text{CH}_4/\text{O}_2/\text{N}_2/\text{CO}_2$  and  $\text{H}_2/\text{O}_2/\text{N}_2/\text{CO}_2$  mixtures. *Int. J. Hydrog. Energy* **34**, 6970 (2009)
- Blanquart, G., Pepiot-Desjardins, P., Pitsch, H.: Chemical mechanism for high temperature combustion of engine relevant fuels with emphasis on soot precursors. *Combust. Flame* **156**, 588 (2009)
- Burke, M., Chaos, M., Ju, Y., Dryer, F., Klippenstein, S.: Comprehensive  $\text{H}_2/\text{O}_2$  kinetic model for high-pressure combustion. *Int. J. Chem. Kinet.* **44**, 444 (2012)
- Cai, L., Pitsch, H.: Optimized chemical mechanism for combustion of gasoline surrogate fuels. *Combust. Flame* **162**, 1623 (2015)
- Cai, L., Minwegen, H., Beeckmann, J., Burke, U., Tripathi, R., Ramalingam, A., Kröger, L., Sudholt, A., Leonhard, K., Klankermayer, J., Heufer, K., Pitsch, H.: Experimental and numerical study of a novel biofuel: 2-butyltetrahydrofuran. *Combust. Flame* **178**, 257 (2017a)
- Cai, L., Kruse, S., Felsmann, D., Thies, C., Yalamanchi, K., Pitsch, H.: Experimental design for discrimination of chemical kinetic models for oxy-methane combustion. *Energy Fuels* **31**, 5533 (2017b)
- Cai, L., Ramalingam, A., Minwegen, H., Heufer, K., Pitsch, H.: Impact of exhaust gas recirculation on ignition delay times of gasoline fuel: an experimental and modeling study. *Proc. Combust. Inst.* **37**, 639 (2019a)
- Cai, L., Minwegen, H., Kruse, S., Ramalingam, A., Hesse, R., Beeckmann, J., Leonhard, K., Heufer, K., Pitsch, H.: Exploring the combustion chemistry of a novel lignocellulose-derived biofuel: cyclopentanol. Part II: experiment, model validation, and functional group analysis. *Combust. Flame* **210**, 134 (2019b)
- Cai, L., Kröger, L., Döntgen, M., Leonhard, K., Narayanaswamy, K., Sarathy, S., Heufer, K., Pitsch, H.: Exploring the combustion chemistry of a novel lignocellulose-derived biofuel: cyclopentanol. Part I: quantum chemistry calculation and kinetic modeling. *Combust. Flame* **210**, 490 (2019c)
- Chan, Y., Zhu, M., Zhang, Z., Liu, P., Zhang, D.: The effect of  $\text{CO}_2$  dilution on the laminar burning velocity of premixed methane/air flames. *Energy Proc.* **75**, 3048 (2015)
- Chen, Z., Qin, X., Xu, B., Ju, Y., Liu, F.: Studies of radiation absorption on flame speed and flammability limit of  $\text{CO}_2$  diluted methane flames at elevated pressures. *Proc. Combust. Inst.* **31**, 2693 (2007)
- de Persis, S., Foucher, F., Pillier, L., Osorio, V., Gokalp, I.: Effects of  $\text{O}_2$  enrichment and  $\text{CO}_2$  dilution on laminar methane flames. *Energy* **55**, 1055 (2013)
- Frenklach, M., Wang, H., Yu, C.L., Goldenberg, M., Bowman, C., Hanson, R., Davidson, D., Chang, E., Smith, G., Golden, D., Gardiner, W., Lissianski, V.: GRI-Mech—an optimized detailed chemical reaction mechanism for methane combustion. <http://combustion.berkeley.edu/gri-mech/> (1999). <http://combustion.berkeley.edu/gri-mech/new21/version12/text12.html>

- Hargis, J., Petersen, E.: Methane ignition in a shock tube with high levels of  $\text{CO}_2$  dilution: consideration of the reflected-shock bifurcation. *Energy Fuels* **29**, 7712 (2015)
- Kim, T., Park, J., Park, H., Park, J., Park, J., Lim, I.: Chemical and radiation effects on flame extinction and  $\text{NO}_x$  formation in oxy-methane combustion diluted with  $\text{CO}_2$ . *Fuel* **177**, 235 (2016)
- Kishore, V., Duhan, N., Ravi, M., Ray, A.: Measurement of adiabatic burning velocity in natural gas like mixtures. *Exp. Therm. Fluid Sci.* **33**, 10 (2008)
- Koroglu, B., Pryor, O., Lopez, J., Nash, L., Vasu, S.: Shock tube ignition delay times and methane time-histories measurements during excess  $\text{CO}_2$  diluted oxy-methane combustion. *Combust. Flame* **164**, 152 (2016)
- Li, X., Jia, L., Onishi, T., Grajetzki, P., Nakamura, H., Tezuka, T., Hasegawa, S., Maruta, K.: Study on stretch extinction limits of  $\text{CH}_4/\text{CO}_2$  versus high temperature  $\text{O}_2/\text{CO}_2$  counterflow non-premixed flames. *Combust. Flame* **161**, 1526 (2014)
- Maruta, K., Abe, K., Hasegawa, S., Maruyama, S., Sato, J.: Extinction characteristics of  $\text{CH}_4/\text{CO}_2$  versus  $\text{O}_2/\text{CO}_2$  counterflow non-premixed flames at elevated pressures up to 0.7 MPa. *Proc. Combust. Inst.* **31**, 1223 (2007)
- Mazas, A., Lacoste, D., Schuller, T.: Experimental and Numerical investigation on the laminar flame speed of  $\text{CH}_4/\text{CO}_2$  mixtures diluted with  $\text{CO}_2$  and  $\text{H}_2\text{O}$ . In: *Proceedings of the ASME Turbo Expo, GT2010-22512* (2010)
- Metcalf, W., Burke, S., Ahmed, S., Curran, H.: A hierarchical and comparative kinetic modeling study of  $\text{C}_1$ - $\text{C}_2$  hydrocarbon and oxygenated fuels. *Int. J. Chem. Kinet.* **45**, 638 (2013)
- Narayanaswamy, K., Blanquart, G., Pitsch, H.: A consistent chemical mechanism for oxidation of substituted aromatic species. *Combust. Flame* **157**, 1879 (2010)
- Narayanaswamy, K., Pitsch, H., Pepiot, P.: A component library framework for deriving kinetic mechanisms for multi-component fuel surrogates: application for jet fuel surrogates. *Combust. Flame* **165**, 288 (2016)
- Pitsch, H.: A C++ computer program for 0D combustion and 1D laminar flame calculations. <http://www.itv.rwth-aachen.de/downloads/flammemaster/> (1990)
- Pryor, O., Koroglu, B., Barak, S., Lopez, J., Ninnemann, E., Nash, L., Vasu, S.: Ignition delay times of high pressure oxy-methane combustion with high levels of  $\text{CO}_2$  dilution. In: *Proceedings of the ASME Turbo Expo, GT2017-63666* (2017)
- San Diego mechanism, Version released on 2014/10/04. <http://web.eng.ucsd.edu/mae/groups/combustion/mechanism.html> (2014). <http://web.stanford.edu/group/haiwanglab/JetSurF/JetSurF2.0/index.html>
- Seshadri, K., Williams, F.: Laminar flow between parallel plates with injection of a reactant at high reynolds number. *Int. J. Heat Mass Transf.* **21**, 251 (1978)